香港中文大學
The Chinese University of Hong Kong

The Chinese University of Hong Kong

Earth System Science Programme

Probability of Occurrence of Strong and Gale Force Winds in Hong Kong During the Passage of Tropical Cyclones

Author:

Chan Ming Hei Kenneth[a]

[a]Department of Physics,
The Chinese University of Hong Kong

Supervisor:

Prof. Tam Chi Yung Francis[a]

Mr. Choy Chun Wing[b]

[a]Earth System Science Programme,
The Chinese University of Hong Kong
[b]Hong Kong Observatory

ESSC4810 Senior Project I

December 9, 2020

Abstract

The Hong Kong Observatory (HKO) issues tropical cyclone warning signals to warn the public of the threat of winds associated with tropical cyclones (TCs). Except the Standby Signal, the other signals are defined based on the wind force in Hong Kong. Statistical methods were applied to correlate the intensity and position of TCs with the probability of occurrence of strong and gale force winds in Hong Kong. A new method was built by mapping the half-hourly positions of TCs with the maximum 10-minute mean wind speed at Cheung Chau (CCH) in the respective previous 30 minutes. The Weibull distribution was applied to estimate the probability of strong and gale force winds at CCH within an area. Results showed that this method could reflect the influence of storm size and strength, wind direction, ridge and monsoon on winds recorded at CCH during TC scenarios. It is hoped that this new method could be extended to other stations in Hong Kong especially newer ones and could assist weather forecasters in assessing the necessity of issuing relevant TC warning signals.

Contents

1 Introduction **4**

2 Literature Review **7**

2.1 Probability forecast tools for strong or gale force winds in Hong Kong . . 7

2.2 Factors affecting local wind strength under tropical cyclone situation . . . 10

2.2.1 Distance to storm centre 10

2.2.2 Storm size 11

2.2.3 Semi-circle effect 11

2.2.4 Terrain 12

2.2.5 Combined effect with other weather systems 12

2.3 Weibull distribution and applications 13

3 Data set **14**

4 Methodology **14**

5 Results **16**

6 Discussion **21**

7 Conclusion **30**

Appendix **33**

List of Acronyms 33

References **34**

List of Figures

1 Gridding of the new “Kidney” method 15

2 Probability Isopleths for Cheung Chau (CCH) 20

3 Super Typhoon Usagi (1319) 22

4 Typhoon Nida (1604); New Gale Kidneys (Red: Typhoon; Blue: Severe Tropical Storm) 23
5 Severe Tropical Storm Jebi (1309); Severe Tropical Storm Strong Wind Kidneys (Cyan: New; Purple: Old) 25
6 Typhoon Kalmaegi (1415); Typhoon Strong Wind Kidneys (Pink: New; Purple: Old) 26
7 Super Typhoon Hato (1713) 28
8 Super Typhoon Mangkhut (1822) 29

List of Tables

1 Hong Kong Tropical Cyclone Warning Signals 5
2 Classification of Tropical Cyclones 14

1 Introduction

Tropical cyclones (TC) threaten the lives and properties in coastal areas by their destructive winds, torrential rain and storm surges (Doocy et al., 2013). Being the most active basin for tropical cyclones, about 30 TCs were generated in the western North Pacific (WNP) annually (Lee et al., 2012). Tropical cyclone warnings have been developed in the Asia-Pacific region to warn the public about the threats brought by TCs to mitigate damage and casualties associated with TCs affecting the territory.

On average, six TCs affect Hong Kong each year (C. C. Lam & Tai, 2004). Since 1917, Hong Kong has been using numbered signal system to give warnings to the local public of wind conditions in Hong Kong under the influence of TCs (C. Y. Lam, 2000). Currently, a five-level warning system is used by the Hong Kong Observatory (HKO). The Standby Signal No. 1 alerts the public that a TC that may affect Hong Kong later is in the vicinity. The higher signals are issued based on the wind speed (and wind direction for the Gale or Storm Signal No. 8) forecast or measured in Hong Kong.

Number	Meaning
1	A TC centred within about 800 km of Hong Kong may affect the territory
3	Strong Wind (41-62 km/h; Beaufort Scale Force 6-7) expected
8[1]	Gale or storm force wind (63-117 km/h; Beaufort Scale Force 8-11) expected
9	Gale or storm force wind expected to increase significantly
10	Hurricane force wind ($\geq$118 km/h; Beaufort Scale Force 12) expected

Table 1: Hong Kong Tropical Cyclone Warning Signals

TC signals are usually issued before local winds are forecast to pick up and reach the designated wind force to allow sufficient lead time for the public to brace for the violent winds and to take relevant precautions. Hence, it is crucial to have forecast tools to assist weather forecasters in issuing timely and precise warnings to minimize loss and damage while avoiding an unnecessary halt of commercial activities which is often unwelcomed by the commercial sectors (C. Y. Lam, 2000), and to avoid lowering the public awareness of typhoon threats due to false alarms.

There are different tools to aid weather forecasters to decide the necessity to issue TC signals. When numerical weather prediction (NWP) models were not maturely developed, statistical guidance could be a useful forecast tool.

The Hong Kong Observatory considered historical TC cases affecting Hong Kong to statistically estimate the probability of occurrence of strong or gale force wind in the Victoria Harbour and other stations. The TC best track data were categorized according to their intensities and locations, and were then mapped back to locally measured wind speeds. The spatial distribution for the probability of occurrence of strong or gale force wind could be estimated for a TC at a specific intensity (C. C. Lam & Tai, 2004; Lee & Ma, 2004).

As NWP models mature and improve in accuracy, numerical model guidance such as meteograms have become important references to weather forecasters, as they predict the time evolution of wind speed and direction for each individual case. Weather forecasters

[1] There are four No. 8 Signals, namely Northeast, Northwest, Southeast and Southwest. Relevant signals are issued when winds are expected to blow from the quarter indicated.

could have a better grasp on the atmospheric condition and could lead to higher confidence in forecasts.

The HKO has developed a method combining statistical and NWP techniques to assess the probability of occurrence of strong or gale force winds in the Victoria Harbour. The method considered the probability of occurrence of strong or gale force winds derived from historical cases by perturbed TC forecast tracks in ensemble prediction systems (EPS). A weighted average of probability was calculated to provide probability forecasts of the Strong Wind Signal No. 3 or the Gale or Storm Signal No. 8. The method was shown to be useful for the issuance and cancellation of relevant TC signals (C. C. Lam & Tai, 2004).

Although the probability forecast tools have been in use for many years, the design of the tools may not be flawless. As the tools were originally designed to aid weather forecasters in issuing and cancelling TC signals, the historical data for the tools only included TCs that necessitated TC signals in Hong Kong. This inevitably included human factors in the statistical guidance. Furthermore, there were limited number of cases for analysis as there were only about six TCs necessitating TC signals in Hong Kong each year, while each of them travelled with different tracks. This could lead to errors in assessing the probability of occurrence of strong or gale force winds due to insufficient data.

In this study, we attempt to eliminate the human factor in the data selection process. We also try to augment the data size and continuity in the data analysis process. It is hoped that this new method could provide a holistic view in the wind situation in Hong Kong under the impact of TCs.

In the next section, the current probability forecast tool will be reviewed. We will also review factors that affect local wind strength under TC scenarios. As we adopted the Weibull distribution in the new method, its characteristics and applications will also be discussed. Our data set and methodology are presented in Section 3 and Section 4 respectively. The study results are presented in Section 5 and discussed in Section 6. The study is finally concluded in Section 7.

2 Literature Review

2.1 Probability forecast tools for strong or gale force winds in Hong Kong

Before numerical weather prediction models were introduced, weather forecasting was mostly based on intuition and experience (Lynch, 2008). Although it might have been imprecise, human forecasters were able to draw empirical rules of thumb to assist them to predict the weather evolution, at least in the short term. This marked the prototype of the analog method of weather forecasting. By recalling a past weather scenario that resembled the present condition, forecasters would predict the present weather scenario would evolve similarly to the past scenario.

The majority of tropical cyclones that affects Hong Kong enters the South China Sea (SCS) from the western North Pacific with a generally northwestward track. Patterns in terms of wind direction veer and wind speed change could be observed for TCs showing similar characteristics.

The Hong Kong Observatory uses a probability forecast tool nicknamed “kidney” to assist weather forecasters in considering the issuance of local TC warning signals. Lee and Ma (2004) illustrated the construction method of the tool. The TC data set included TCs that necessitated the issuance of the Strong Wind Signal No. 3 or higher signals and led to gales in the Victoria Harbour. Data were checked when the Signal No. 3 or higher signals were in force. The onset and cessation of gales in the Victoria Harbour were defined as the first and the last occurrence of gales (10-minute mean wind) at any of the eight stations around the harbour. There were some TCs in the data set, mainly in autumn and winter, being manually excluded. This was because the occurrence of gales were judged to be attributed significantly to the effect of the prevailing northeast monsoon such that gales were recorded in the harbour despite the TC being far away from Hong Kong.

The rest of the TCs was classified according to their intensities. For each 1°× 1° square within 15°- 26°N, 106°- 123°E, the number of TCs of each intensity class passing the square was counted. The percentage of TCs causing gales in each square could be calculated. Finally, probability isopleths describing the likelihood of occurrence of gales

in the harbour when a TC of certain intensity was centred in a location in the SCS could be plotted.

The probability isopleths for severe tropical storms and typhoons were manually constructed. Two tropical storm cases were merged into the STS cases due to the small sample size. However, the sample sizes for T and STS were still small as there were only 32 TCs that caused gales in the harbour in the study period. The gridding of the squares was also rough. The isopleths were hence subjectively smoothed following certain empirical rules.

For isopleths of the same probability, the isopleth corresponding to a cyclone stronger in intensity should envelop those for weaker cyclones, while their shapes should largely be similar. Probability isopleths for strong winds or other stations could be constructed in a similar manner.

The isopleths showed distinctive characteristics. They were elongated towards the southwest and had tight gradients on the eastern and southeastern sides. This was due to the degree of exposure of the harbour. Easterly winds were not sheltered while winds from the north were hindered by hills. The difference will be further illustrated in the next subsection. The tool was given a nickname "pig kidney" or simply "kidney" due to the southwestward elongation feature.

Ensemble forecasts, either using the ensemble prediction system of a single model by perturbing the initial conditions or using a set of independent numerical models, have been proven to be more skillful than single model forecasts (Aberson, 2001; Elsberry & Carr, 2000; Weber, 2003; Zhang & Krishnamurti, 1997). C. C. Lam and Tai (2004) introduced a method to further improve the assessment of TC signals. The HKO input the TC forecast tracks from several NWP models to generate an ensemble forecast track. Taking the HKO warning track error and the deviations of the TC forecast positions of individual models into consideration, 25 perturbed tracks were generated to represent different possible scenarios. A bivariate Gaussian distribution was adopted to fit the perturbation field. The probability density function (PDF) for the TC to occur in a position could then be obtained.

One may then calculate the probability of occurrence of strong or gale force winds (in

the Victoria Harbour) at time t. The probability $P(t)$ is given by:

$$P(t) = \sum_{k=1}^{25} P_I(W \mid r_k) P(r_k(t)) \tag{1}$$

where $P_I(W \mid r_k)$ denotes the probability of strong or gale winds given the location of TC at r on the k^{th} perturbed track and intensity category I. The probability was derived from the respective "kidneys". $P(r_k(t))$ represents the probability of the TC at location r and time t on the k^{th} perturbed track. The time evolution of probability of strong or gale winds was easily visualized and the tool was found to be useful for the issuance and cancellation of relevant TC signals.

Lam and Tai also discussed the limitations of the tool. The intensity stratification was not fine enough. When the intensity of the TC changed, the probability of strong or gale winds might abruptly change. The errors in intensity forecast were not catered, which might lead to inaccurate assessment of wind evolution when unexpected intensity change occurred. The effect on storm size and the combined effect of northeast monsoon were not considered in constructing the probability isopleths. Weather forecasters would have to be careful in using the tool, especially when the wind radii of the TC was abnormally large, which would lead to the early onset of strong or gale winds.

Furthermore, the construction process of the probability isopleths was highly subjective. The sample size was not large. There were only 32 TCs leading to gales in the Victoria Harbour in the study period. The sample size in each $1° \times 1°$ square would be even smaller as TCs traversed with unique tracks. The calculated probability might be of large error and uncertainty. There was also a lack of continuity in finding the spatial distribution of probability values as there was no overlap between two neighbouring grid squares. It highly relied on one's perception and intuition in drawing the probability isopleths.

Economic activities are no longer confined along the coast of the Victoria Harbour under new town development schemes in Hong Kong. It is necessary to study the wind characteristics at other anaemometer stations. However, the data selection process of Lee and Ma's method involves a significant human factor: TC warning signals. The data set only includes TC and local wind data when the No. 3 or higher signals were in force. The HKO considers the overall winds in Hong Kong when issuing relevant TC signals. Certain

offshore and coastal stations may be more windy as they are less sheltered. However, relevant signals might not be issued when winds in other regions are not forecast to pick up significantly. Signals may also be cancelled early when local winds start to moderate but offshore winds are still strong.

To construct a better probability map for different stations, one may search for a method to augment the sample size without compromising the authenticity of the data, while the human factor should also be minimized.

2.2 Factors affecting local wind strength under tropical cyclone situation

There are many factors that contribute to the local wind speed at different stations in Hong Kong. The track and intensity of TCs can only provide a general description of the wind speed evolution in Hong Kong, but they are insufficient to fully explain the local observations.

2.2.1 Distance to storm centre

The Rankine vortex is often adopted to describe the structure of tropical cyclones (Katopodes, 2019). The mathematical expression of the Rankine vortex is given by:

$$v_\theta = \begin{cases} \Omega_0 r, r \leq R \\ \frac{C}{r}, r > R \end{cases} \tag{2}$$

where r is the radial distance from the vortex centre, R defines the radius of the rigid rotating core, Ω_0 is the angular velocity of the core and $C = R^2\Omega_0$ is the strength of the vortex.

As a rule of thumb, local winds are stronger when the TC centre is closer to Hong Kong. Statistically, it was rare for a TC skirting about 350 km or further from Hong Kong to cause general gales in the territory (Shum & Or, 2012). For weaker TCs such as tropical storms, they usually need to be very close or pass directly over Hong Kong to cause gales in Hong Kong (C. C. Lam & Tai, 2004).

2.2.2 Storm size

The extensiveness of high winds due to a TC is determined by its storm size. Storm size is quantified ideally according to the radius of zero tangential winds (Bender et al., 2017; Knaff & Zehr, 2007). However, it is difficult to obtain an accurate estimate of storm size with this metric. Operationally, it is more convenient to define storm size as the radius of the outermost closed isobar (Knaff & Zehr, 2007; Lee & Ma, 2004; Sun et al., 2015; Zhai & Jiang, 2014). It is also useful to measure the radial extent of certain levels of winds (Bender et al., 2017; Knaff & Zehr, 2007; Nam et al., 2018; Shum & Or, 2012; Zhai & Jiang, 2014), especially when TC warnings are related to the local wind strength. There may be differences in wind radii at different quadrants of a TC, and they are conspicuous when the pressure gradient is tightened due to the existence of other prominent weather systems such as monsoons or ridges. Weaker TCs may have non-uniform development around the storm size so that significant convections and rainbands may be tilted to one side or one quadrant. Moreover, TCs moving at high speed may result in significant semi-circle effect which causes the wind radii to differ along the axis of traverse. In general, storms with larger wind radii can bring high winds to Hong Kong relatively early during their approach or when they skirt at a greater distance from Hong Kong.

2.2.3 Semi-circle effect

The semi-circle effect refers to the result of the superposition of the rotational wind field of the TC and its translation speed. In the northern hemisphere, the rotational wind field and the translation speed are additive on the right side of the TC, while the translation is counter-directional to the rotational wind on the left side of the TC (Nam et al., 2018). The right side of the TC, with respect to its direction of movement, is called the dangerous semicircle due to a higher wind speed. The left side is referred to as the navigable semi-circle where winds are less violent. The semicircle effect is more significant when the TC traverses with high speed.

2.2.4 Terrain

Terrain can serve as shelter which leads to the decrease in local wind speed. Due to urbanization, many high-rise buildings have been constructed in Hong Kong which cause obstruction of air flow. There are also hills to the north and the south of the Victoria Harbour, and such orographic setting of the Harbour causes it to be more exposed to easterly winds (Lee & Ma, 2004). For important reference stations, the Observatory has been surrounded by high-rise buildings since 1958, leading to a decrease in measured wind speed. As such, it is no longer valid to use the Observatory's winds to assess the general wind situation near sea-level (Chin & Leong, 1978). For Cheung Chau station, which is the main focus of this study, it is observed that it is most prone to northerly winds and east to southeasterly winds while it is less sensitive to northeasterly winds, likely due to the existence of mountains to its north and east (Shu et al., 2015).

However, valleys or alignment of buildings may lead to amplification in wind speed by the wind tunnel effect or the valley effect. The valley effect happens when air flows from an open area into a narrow valley. The air movement is accelerated due to the accumulation of air in the valley, resulting in a higher wind speed in the valley (Yang, 2014). The valley effect can be observed in settings of both natural terrain and urban fabric, where high wind speed may be observed along streets with high-rise buildings when the alignment of the buildings creates a "valley" in the street canyon. During the approach of Typhoon York in September 1999, many curtain walls were broken on towers in Wan Chai North due to the high winds and amplified wind pressure under the valley effect (K. M. Lam et al., 2006). The valley effect may pose extra threat to the safety of citizens and building structures.

2.2.5 Combined effect with other weather systems

The existence of other weather systems may tighten the pressure gradient along the coast of southern China and may cause local winds in Hong Kong to further strengthen during the approach of a TC. The most common situation for such combined effect is the rendezvous of the northeast monsoon with a TC in the South China Sea, and the presence of northeast monsoon can lead to the early onset of gales in Hong Kong when the TC is still far away (Lee & Ma, 2004).

2.3 Weibull distribution and applications

The Weibull distribution can fit into widely diverse kinds of random phenomena ("Properties of the Weibull Distribution", 2012), and can be used to assess product life. It is also widely adopted by literature to analyze local wind characteristics for wind energy-related assessments due to its remarkable resemblance in actual wind distribution (Ali et al., 2018; Azad et al., 2019; Bilir et al., 2015; Gryning et al., 2016; Ozay & Celiktas, 2016; Shu et al., 2015; Ucar & Balo, 2009). The data-logging of the wind data was in one-minute or ten-minute intervals. The cumulative distribution function (CDF) of the Weibull distribution is given by:

$$F(x) = 1 - e^{-(\frac{x-\gamma}{\lambda})^k}; x > \gamma \tag{3}$$

where γ is the location parameter or the threshold parameter, represents the guarantee time in life testing applications ("Properties of the Weibull Distribution", 2012). However, for wind distribution the value of γ is normally set to zero as there does not exist a minimum wind speed. The function then reduces to the more common two-parameter Weibull distribution. $\lambda > 0$ is the scale parameter, also known the characteristic value. $k > 0$ is the shape parameter and when $k = 1$ the distribution reduces to nothing but the exponential distribution.

The PDF $f(x; \lambda, k)$ is simply $\frac{dF(x)}{dx}$. It is given by:

$$f(x; \lambda, k) = \frac{dF(x)}{dx} = \frac{k}{\lambda}(\frac{x}{\lambda})^{k-1} e^{-(\frac{x}{\lambda})^k} \tag{4}$$

The reliability function $R(x)$ gives the probability of the exceedance of a given value x for a quantity following the Weibull distribution. It has the form

$$R(x) = e^{-(\frac{x-\gamma}{\lambda})^k}; x > 0. \tag{5}$$

If we obtain the scale and shape parameters of a distribution representing the wind characteristics at a station, it is easy to estimate the probability of wind exceeding a certain threshold.

3 Data set

This research included tropical cyclones within 15°- 26°N, 106°- 123°E from 1993 to 2018. The intensity and position data were based on the Hong Kong Observatory (HKO) best track data. The raw data was in 6-hourly intervals at 00, 06, 12 and 18 UTC. The positions of TCs were linearly interpolated to half-hourly intervals. No interpolation was done for the intensity data. Instead, the half-hourly intensity data followed the raw intensity data just prior to the given time. The data was then matched to the maximum 10-minute sustained wind speed recorded at Cheung Chau (CCH) in the respective previous 30 minutes. If multiple TCs existed in the region, manual judgement was made to determine which TC was the major contributor to the winds in Hong Kong.

4 Methodology

The TC data was first categorized according to their intensities. There were four categories, including tropical depression (TD), tropical storm (TS), severe tropical storm (STS) and typhoon (T).

Classification	Maximum 10-minute mean wind near the centre	
	km/h	knots
Tropical Depression (TD)	41-62	22-33
Tropical Storm (TS)	63-87	34-47
Severe Tropical Storm (STS)	88-117	48-63
Typhoon (TY)	$\geq$118	$\geq$64

Table 2: Classification of Tropical Cyclones

The TC data and the corresponding wind speed data at CCH in each 1°$\times$ 1° square within 15°- 26°N, 106°- 123°E were analyzed. To enhance the continuity in the spatial distribution of probability of high winds, we used "running" 1°$\times$ 1° squares where the squares were centred at x.5°N, x.5°E (red squares in Figure 1) or x.0°N, x.0°E (blue squares in Figure 1).

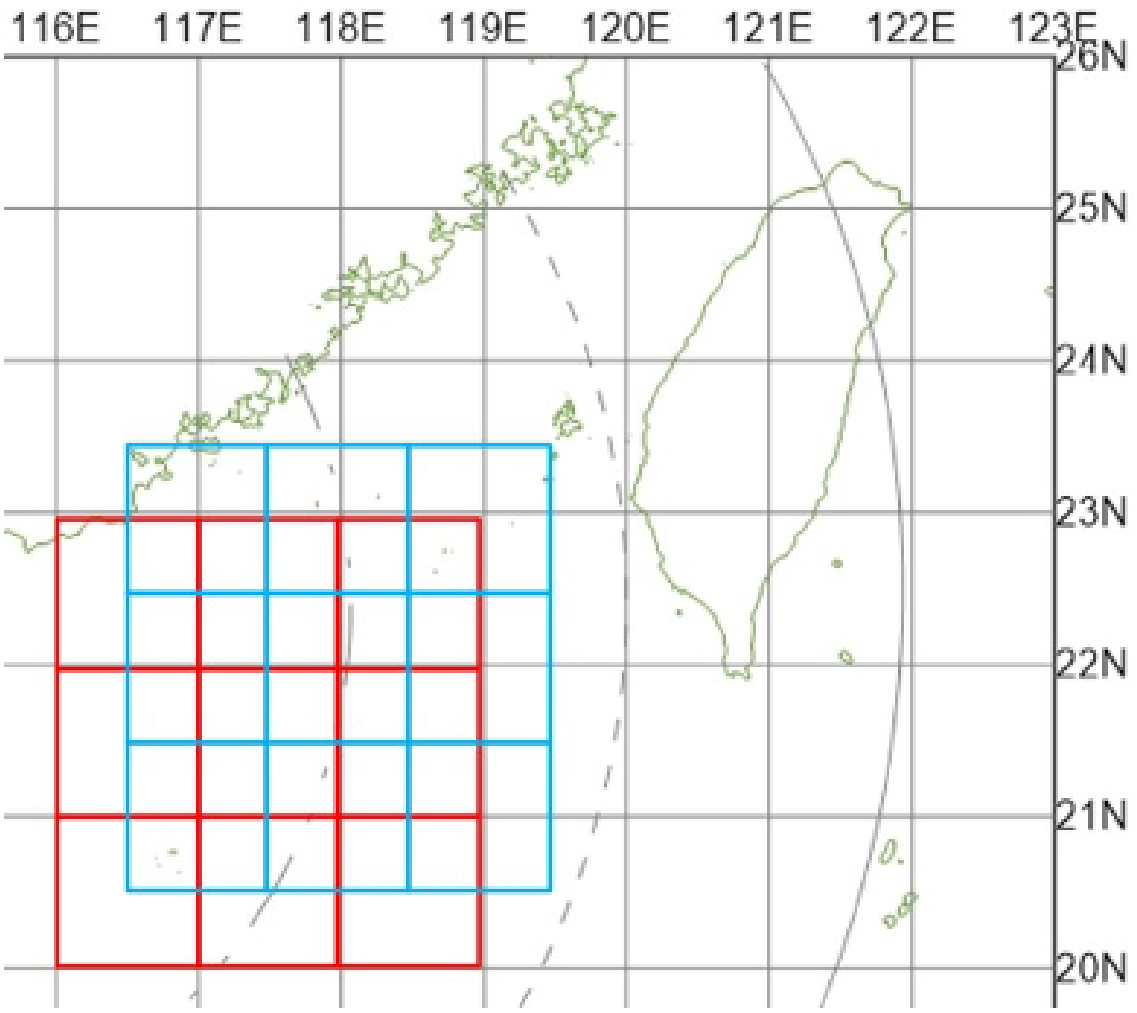

Figure 1: Gridding of the new “Kidney” method

TCs traverse at different speeds and with unique trajectories. In general, slow-moving TCs may contribute more data in a grid square as they stay in the square for a longer period. Fast-moving TCs or TCs skimming the grid square contribute less data in a grid square.

To ensure fairness in which each TC makes equal contribution to each square, the number of data retained for each TC in the square was reduced to that of the TC with the least data in that square. The data with the highest wind speed recorded at CCH was kept for each TC and the excess data with lower wind speed was discarded.

After the data selection process, if there were at least 10 pieces of data left in the grid square, the CCH wind speed data would be fit with the Weibull distribution, given by:

$$f(x;\lambda,k) = \begin{cases} \frac{k}{\lambda}(\frac{x}{\lambda})^{k-1}e^{-(\frac{x}{\lambda})^k}, & x \geq 0 \\ 0, & x < 0 \end{cases} \tag{6}$$

where $k > 0$ is the shape parameter and $\lambda > 0$ is the scale parameter. Upon proper data fitting, the probability of winds to exceed 11.4 m/s (Beaufort Scale Force 6) or 17.5 m/s (Beaufort Scale Force 8) could be calculated respectively from the distribution, using the reliability function $R(x)$ as given in Equation 5.

After calculating the probability of strong and gale winds for each grid square in each category, probability isopleths were plotted using Surfer.

5 Results

The strong and gale isopleths were plotted for the four categories. Since tropical depressions do not lead to local gale winds theoretically, the gale isopleths for tropical depressions were not presented.

Figures 2a-g show the probability isopleths generated by Surfer. The raw probability values calculated by the fitted Weibull distributions were overlaid on the maps.

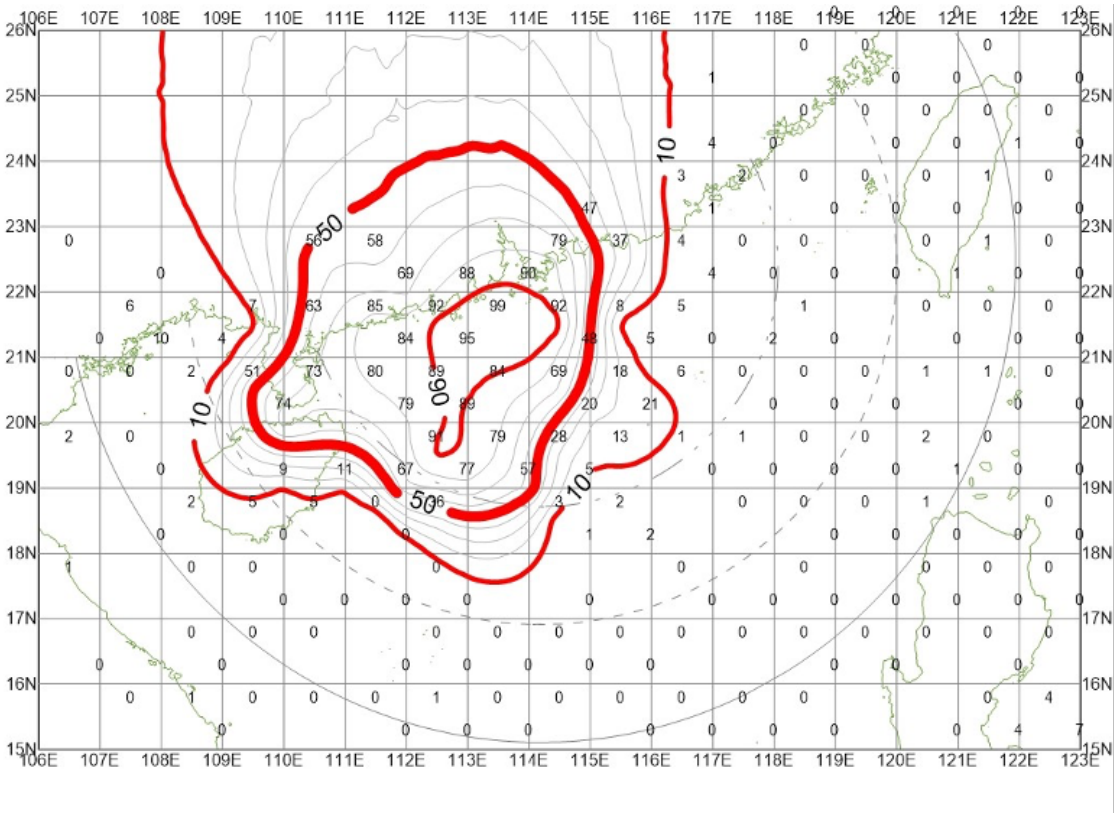

(a) Probability Isopleths of Gale Winds for Typhoons

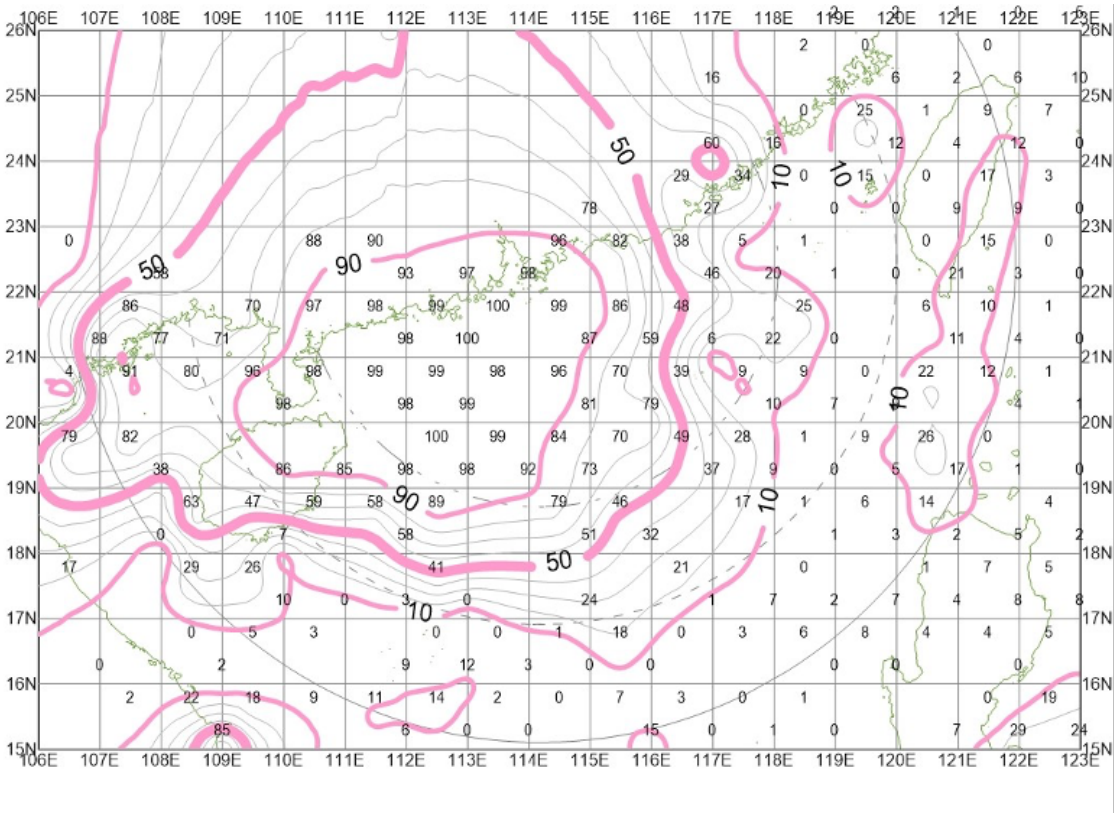

(b) Probability Isopleths of Strong Winds for Typhoons

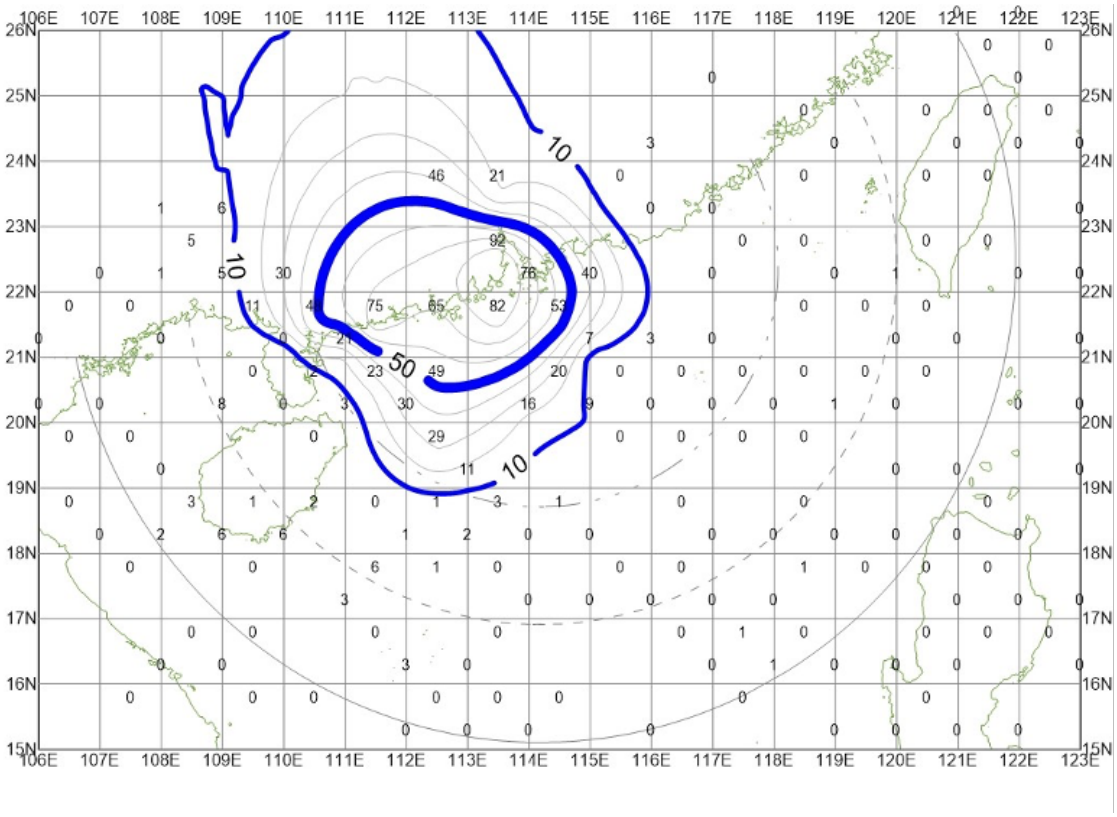

(c) Probability Isopleths of Gale Winds for Severe Tropical Storms

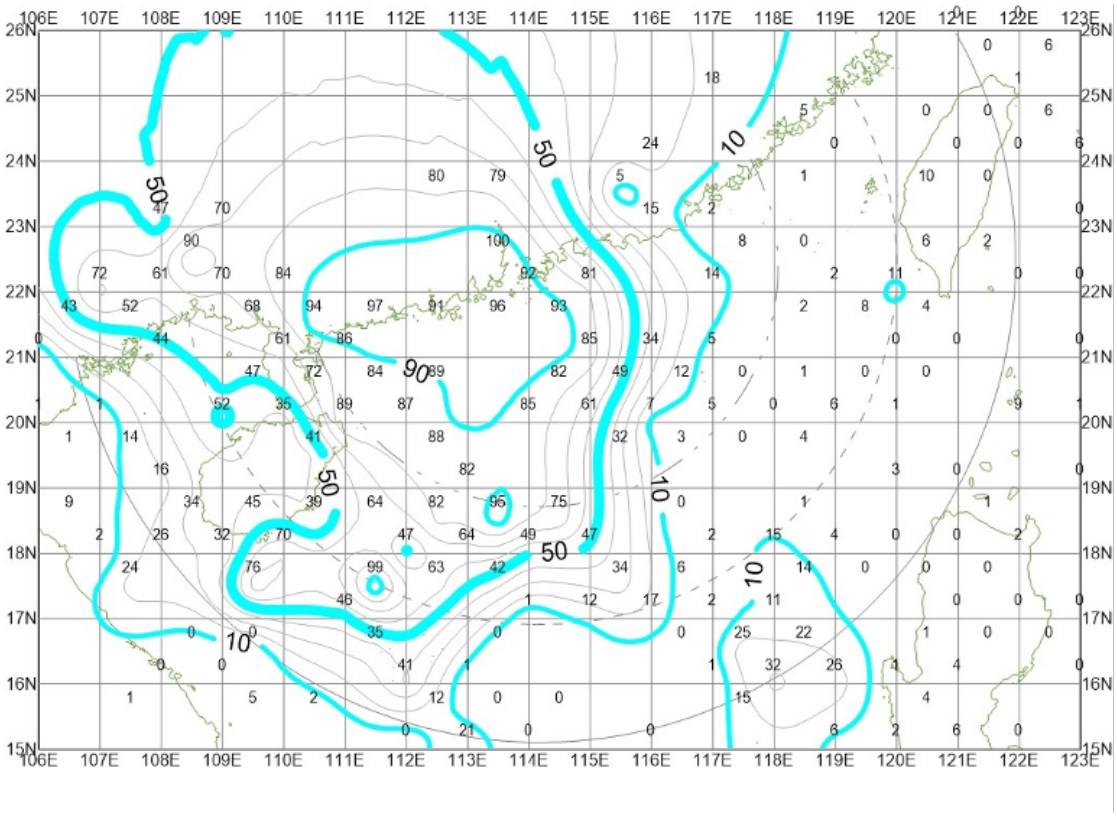

(d) Probability Isopleths of Strong Winds for Severe Tropical Storms

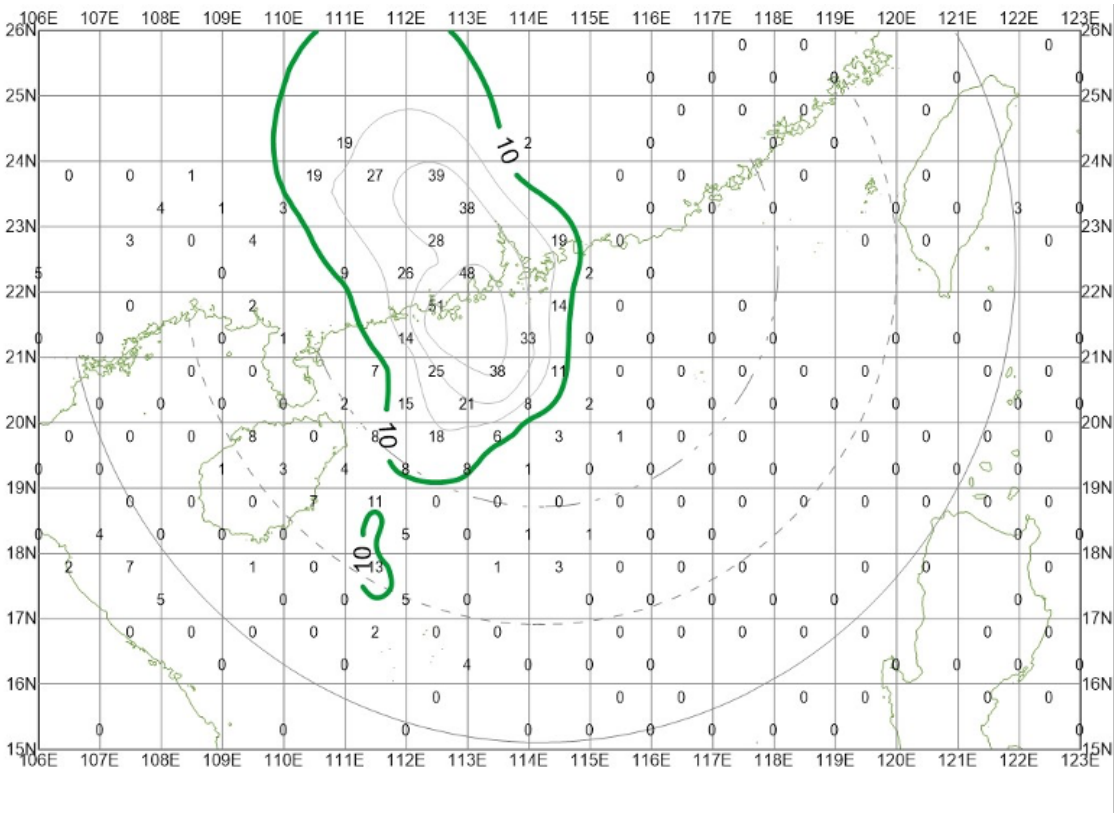

(e) Probability Isopleths of Gale Winds for Tropical Storms

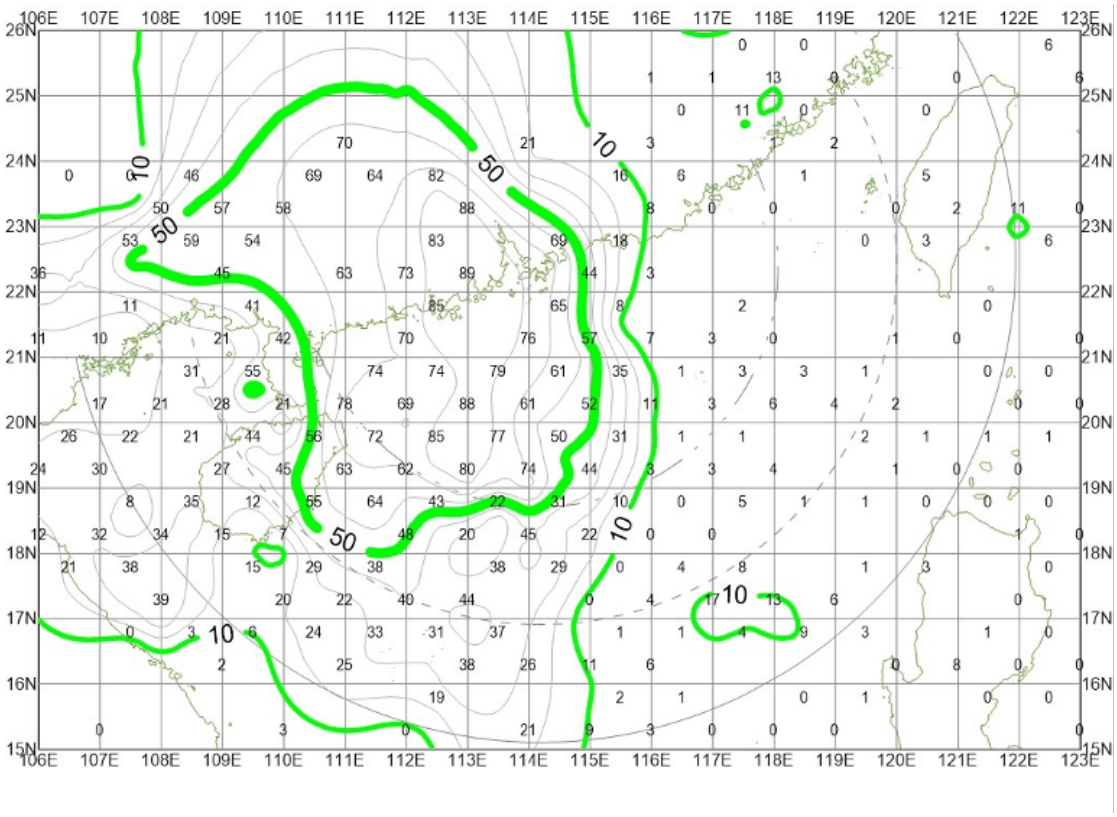

(f) Probability Isopleths of Strong Winds for Tropical Storms

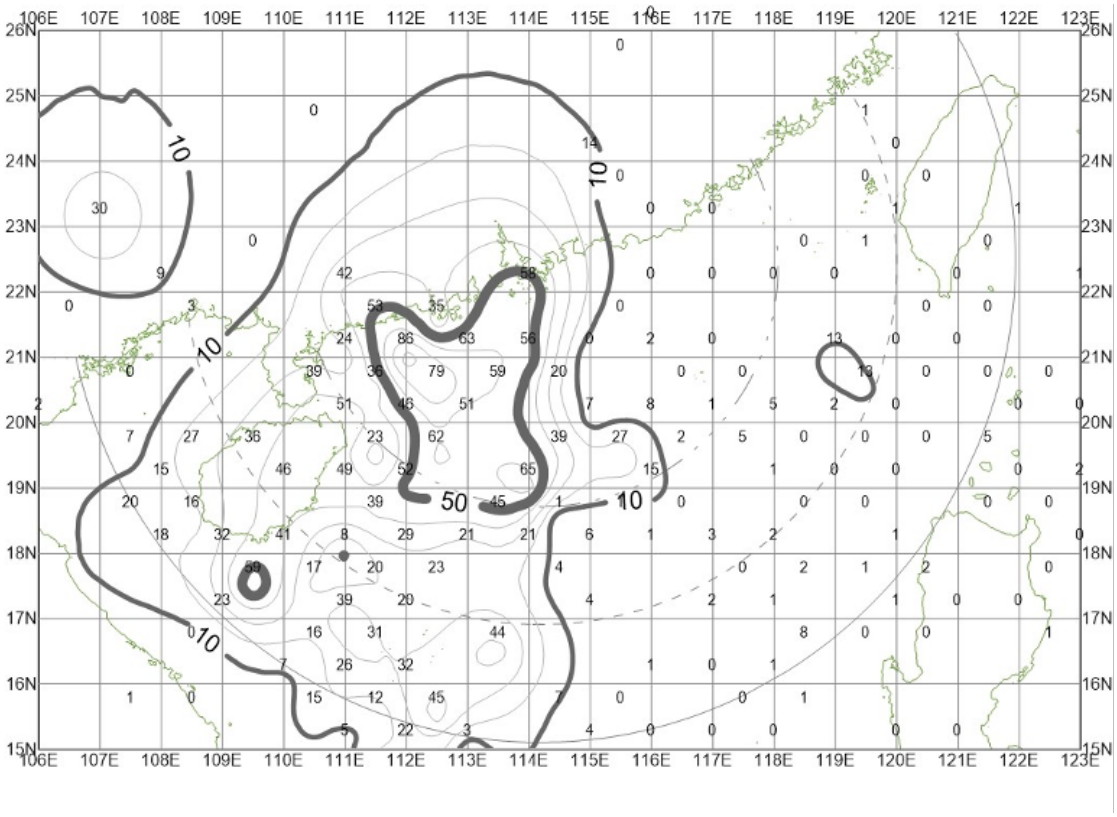

(g) Probability Isopleths of Strong Winds for Tropical Depressions

Figure 2: Probability Isopleths for Cheung Chau (CCH)

It should be noted that the sections of isopleths that extended northwards to the inland area were less reliable as there was insufficient TC data inland.

6 Discussion

When compared to the original "kidneys", the new "kidneys" showed various similarities and differences.

Both versions of "kidneys" were less extensive to the east of Hong Kong than to the west and have steeper gradients. It reflected that northerly winds at CCH were generally sheltered by terrain when a TC approached from the east. Winds picked up to strong (F6) or gale (F8) force only when the TC came close to the coast. Figures 3 and 4 show the tracks of two typhoons that approached Hong Kong from the east and made landfall to the east of Hong Kong. In both cases, winds veered in a counterclockwise direction from northerlies, then to northwesterlies and finally southwesterlies. It could be observed that winds became persistently strong (yellow circles) only when the typhoon was some 200 kilometres from Hong Kong. Gale force winds (red circles) were recorded when the typhoon was directly hitting Hong Kong (within 100 kilometres from HKO). For Super Typhoon Usagi, winds picked up slightly earlier when the storm was crossing the respective 30% probability isopleths. The relatively large storm size of Usagi was accountable for the early onset of high winds.

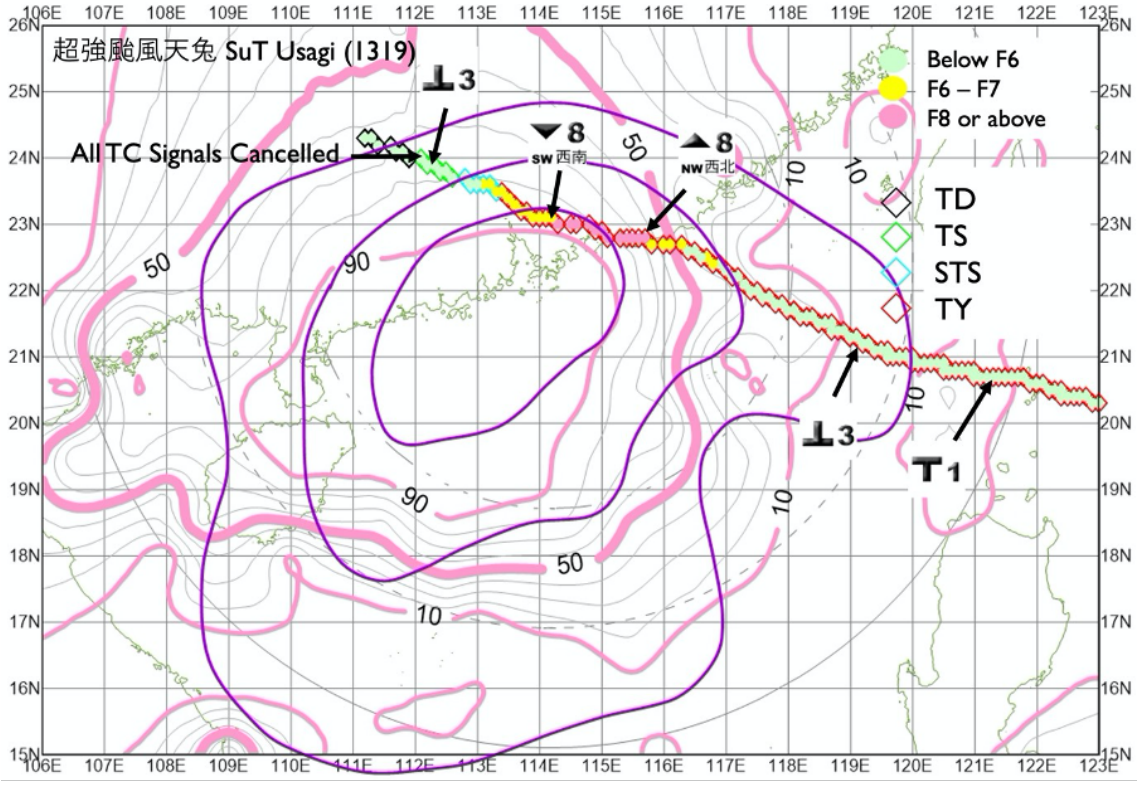

(a) Typhoon Strong Wind Kidneys (Pink: New; Purple: Old)

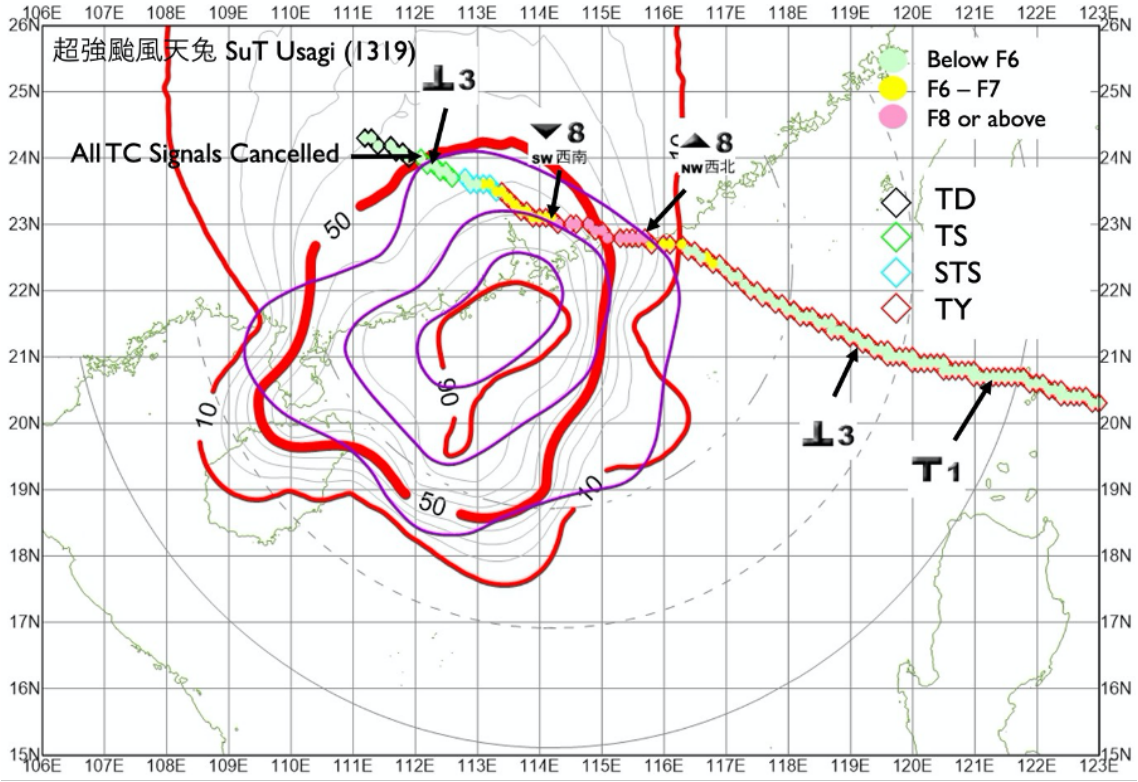

(b) Typhoon Gale Kidneys (Red: New; Purple: Old)

Figure 3: Super Typhoon Usagi (1319)

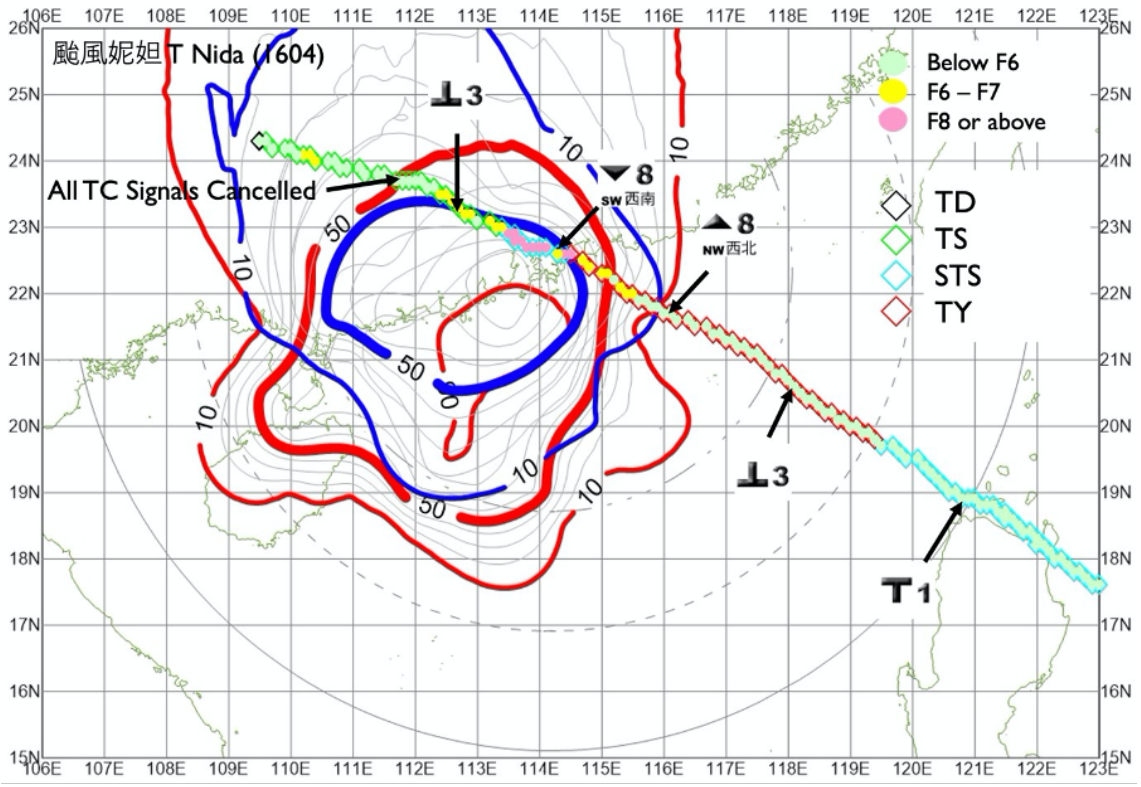

Figure 4: Typhoon Nida (1604); New Gale Kidneys (Red: Typhoon; Blue: Severe Tropical Storm)

In both the old and new versions of "kidneys", axes of maximum probability pointing to the southwest of Hong Kong were observed, where easterly to southeasterly winds dominate. Winds in Hong Kong during TC scenarios are generally strongest when winds blow from the southeast. This agrees with the literature, reflecting that Hong Kong is more vulnerable to winds from the southeastern quadrant. Furthermore, the semi-circle effect due to northwestward-moving TCs may also amplify the easterly winds. Semi-circle effect is more prominent in TCs with high translation speed. The onset of strong or gale force winds may be early when the track cuts the low probability isopleths.

In some of the new "kidneys" including the strong wind "kidneys" for typhoons, severe tropical storms and tropical storms, one may notice there is another axis of maximum probability extending to the west of Hong Kong (excluding the unreliable ridge to the north). This is likely due to high sensitivity to southeasterly winds of CCH due to its exposure to the southeast.

The isopleths of the new "kidneys" are more extensive in the southwestern quadrant when compared to the old "kidneys". The difference may be due to the early cancellation of TC signals during a TC's departure, or the issuance of the Strong Monsoon Signal instead of TC signals when the strong winds were due to the combined effect of northeast monsoon or ridge and a TC in the SCS. In the old "kidneys", these sections of TC tracks were not included and may have led to an underestimation in the threat of strong winds.

Figures 5 and 6 show two storms that necessitated TC signals in Hong Kong followed by the SMS. Under the combined effect of the subtropical ridge and the TC, strong south-easterly winds were recorded at CCH even though the TC was already distant from Hong Kong. For both STS Jebi and T Kalmaegi, the sections of strong winds in the Gulf of Tonkin were out of the 10% isopleths for old "kidneys", while they were enveloped by the 50% isopleths of the new "kidneys", which reflected the influence of the ridge. As segments of TC tracks when no TC signals were in force were neglected in constructing old "kidneys", the sensitivity to southeasterly winds of CCH when TC departs further to the west or due to the combined effect could not be reflected in old "kidneys".

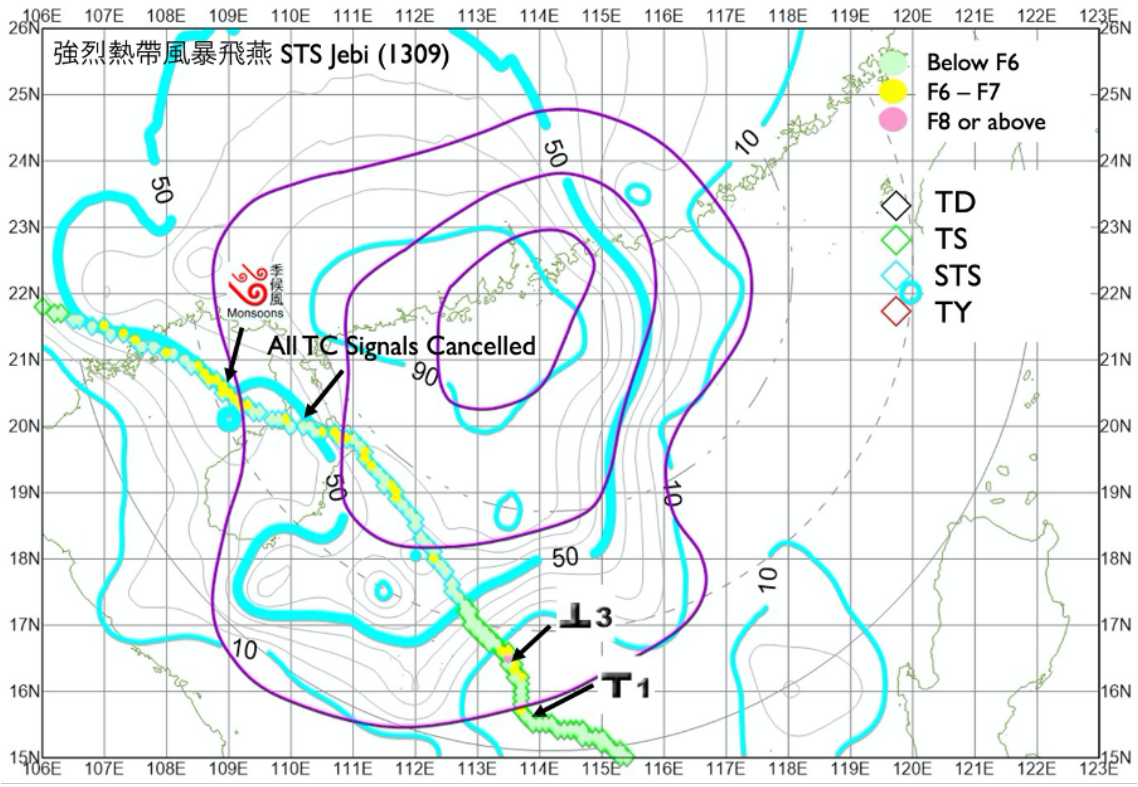

Figure 5: Severe Tropical Storm Jebi (1309); Severe Tropical Storm Strong Wind Kidneys (Cyan: New; Purple: Old)

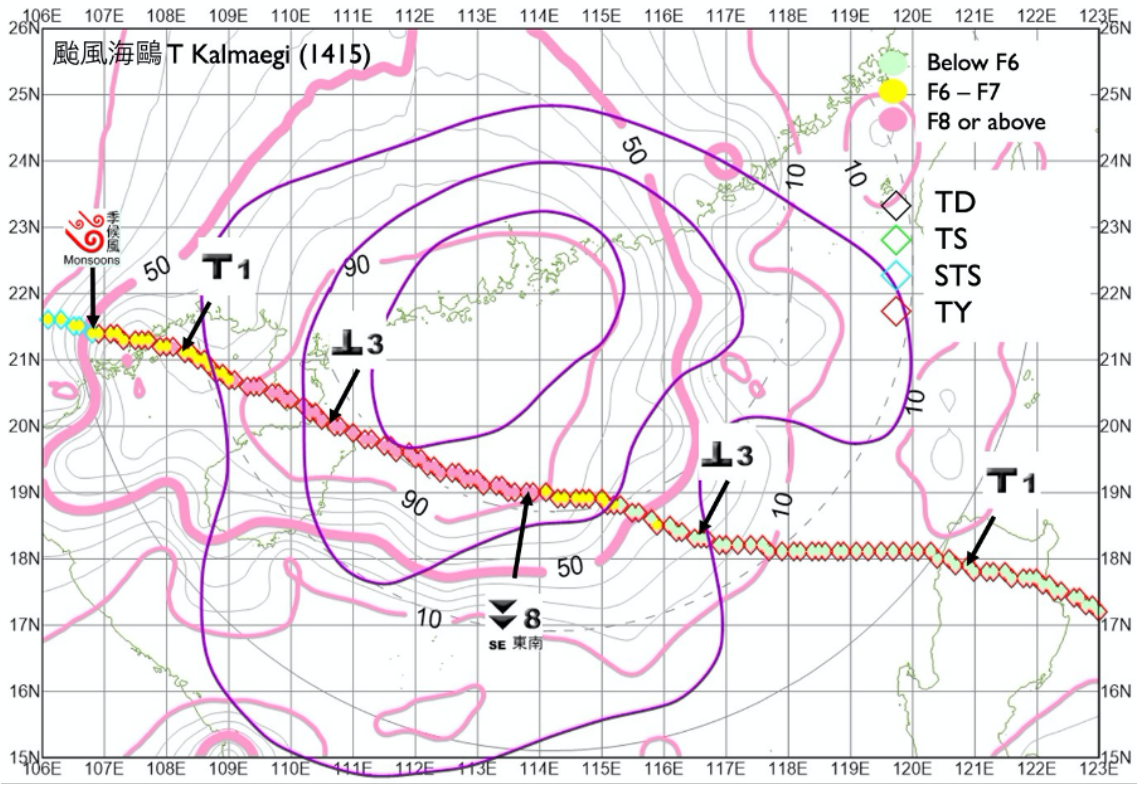

Figure 6: Typhoon Kalmaegi (1415); Typhoon Strong Wind Kidneys (Pink: New; Purple: Old)

The new set of "kidneys" are also able to reflect the effect of storm size on the onset time of strong and gale force winds at Cheung Chau. Midget TCs or TCs with tight wind radii lead to late onset of high winds while TCs with large storm size or extensive wind radii lead to early onset of fierce winds.

Figures 7 and 8 show the tracks of Super Typhoon Hato in 2017 and Super Typhoon Mangkhut in 2018 respectively. Both super typhoons necessitated the Hurricane Signal, No. 10 in Hong Kong. Hurricane force winds were recorded at CCH during the approach of both storms.

Hato attained a peak intensity 100 knots near its centre, yet it had very tight wind radii. Its gale radius was only 90 nm during its closest approach to HKO. As shown in Figures 7a and 7b, not until Hato entered the respective 90% probability envelope did winds at Cheung Chau pick up to strong or gale force. Since Hato had tight wind radii, winds soared when Hato came close to Hong Kong and plunged soon after it made landfall at Zhuhai.

Mangkhut had a large storm size. Its strong and gale wind radii reached 330 nm and 225 nm respectively during its closest approach to HKO. As a result, winds at Cheung Chau picked up relatively early when Mangkhut was still far away from Hong Kong. As shown in Figures 8a and 8b, strong winds and gale winds were first recorded soon after Mangkhut's track intersected with the 10% probability isopleths when Mangkhut was edging closer to Hong Kong. Since the circulation of Mangkhut was broad, the rate of change in local wind speed was less rapid than that during Hato's approach. Gale winds were recorded at Cheung Chau for over a day owing to the extensive wind radii of Mangkhut. The rate of change in wind speed was also less abrupt.

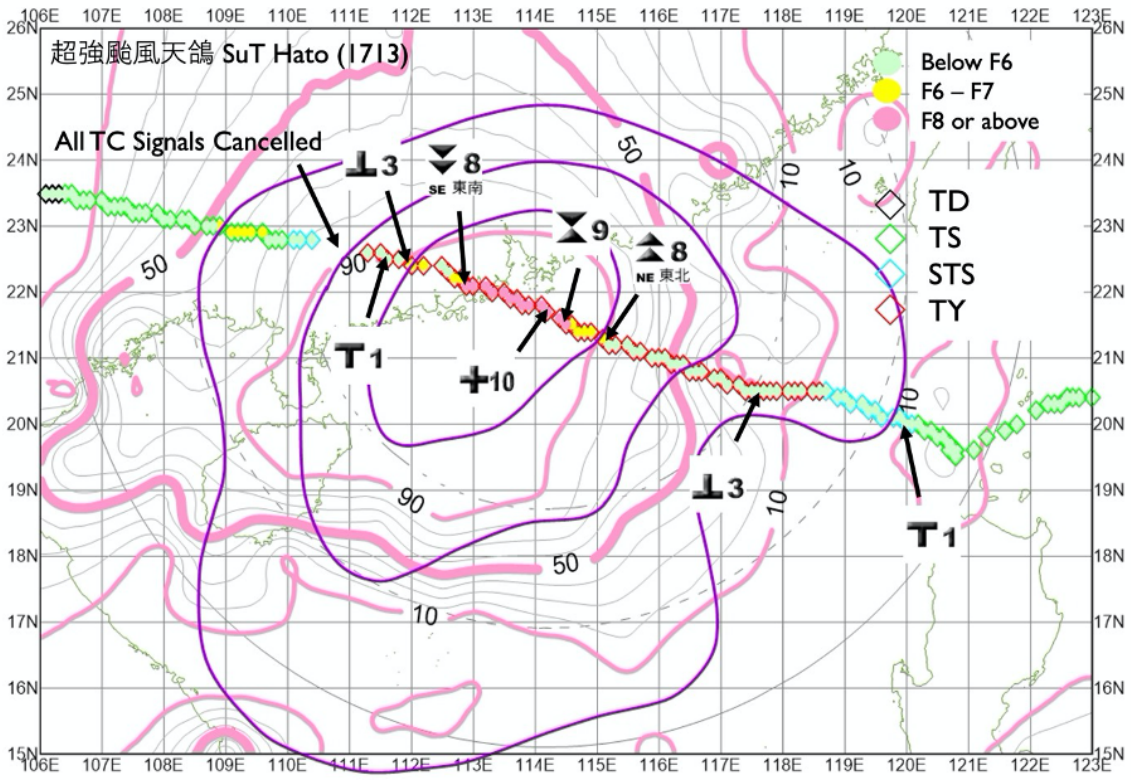

(a) Typhoon Strong Wind Kidneys (Pink: New; Purple: Old)

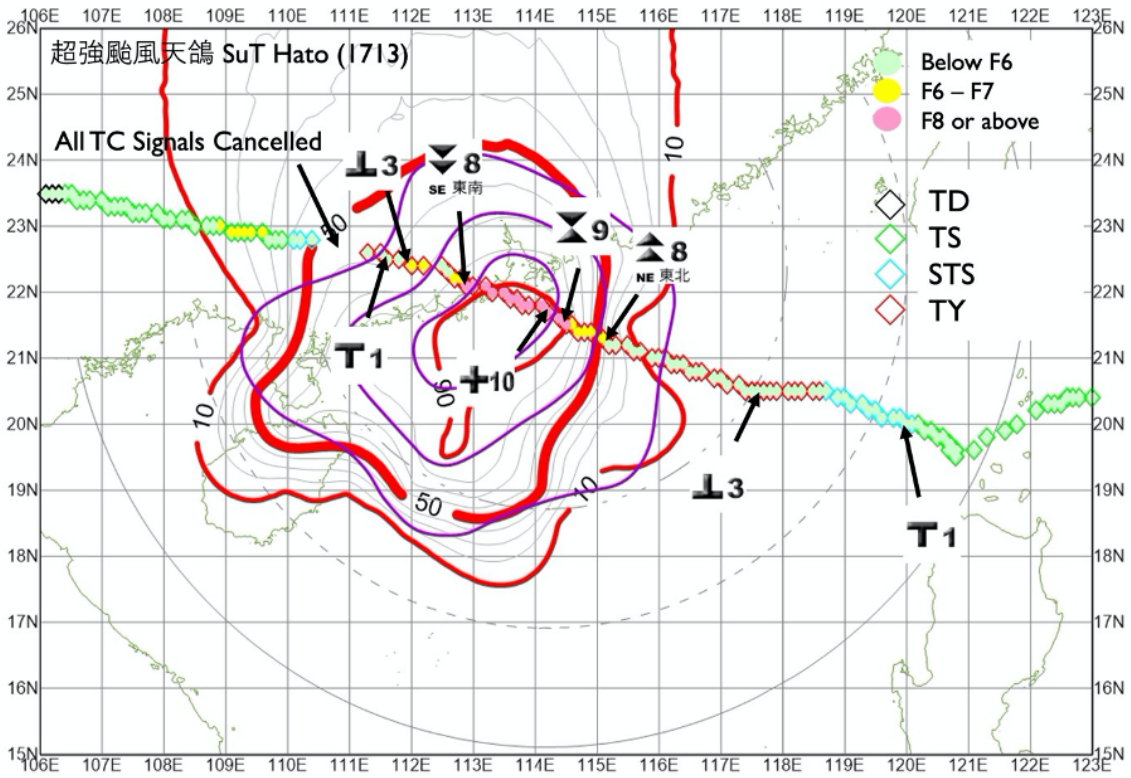

(b) Typhoon Gale Kidneys (Red: New; Purple: Old)

Figure 7: Super Typhoon Hato (1713)

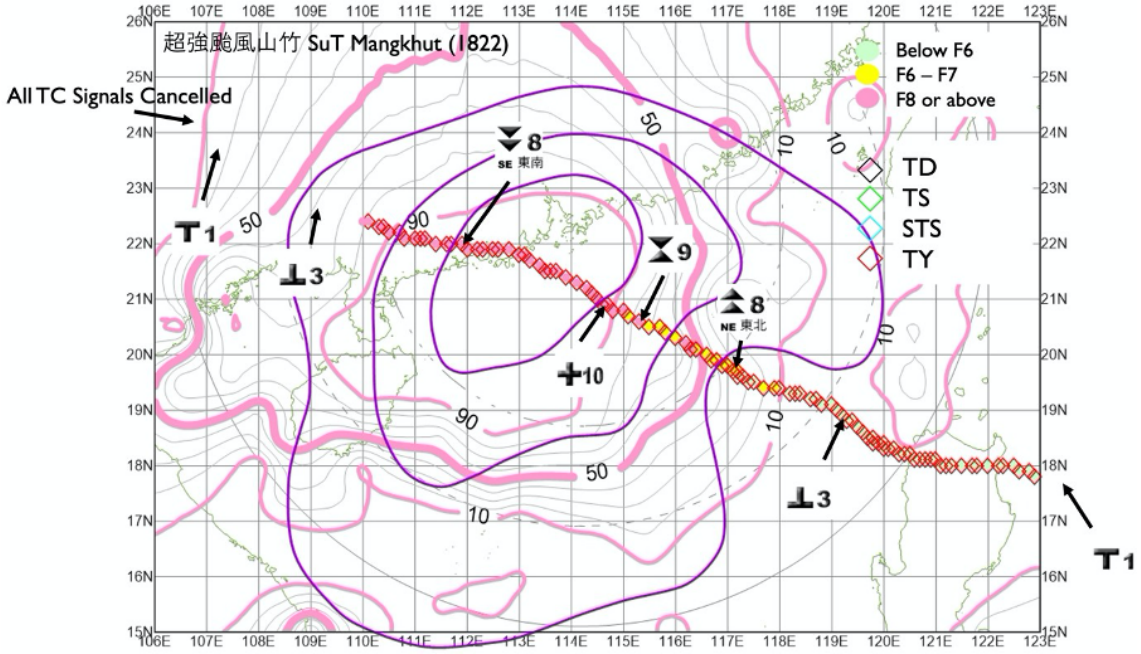

(a) Typhoon Strong Wind Kidneys (Pink: New; Purple: Old)

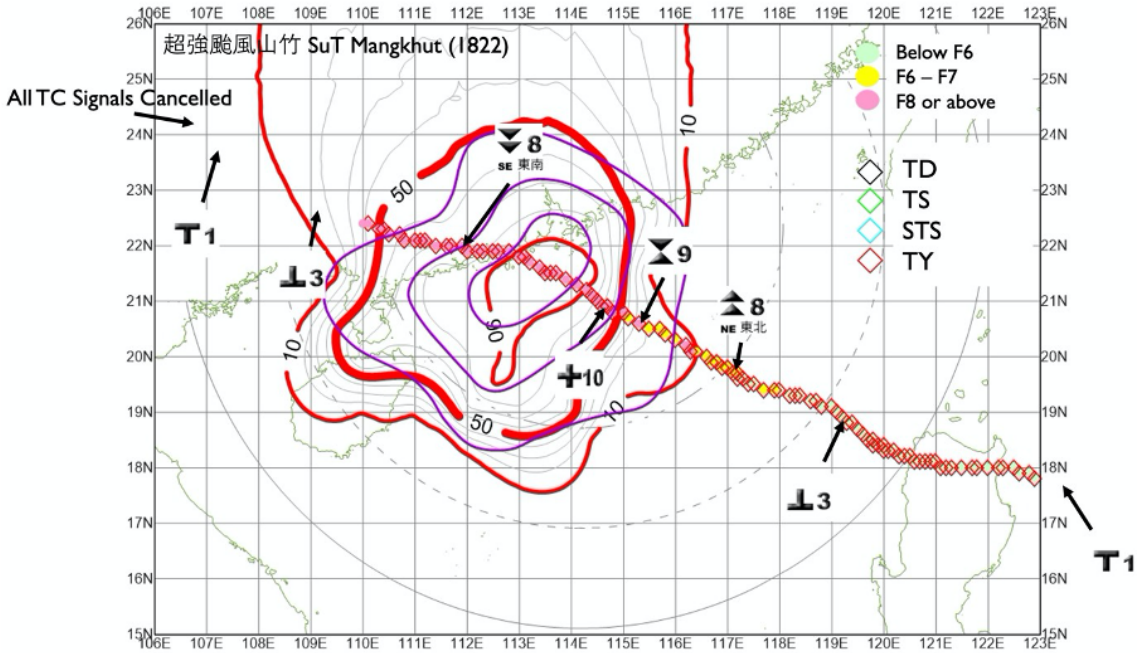

(b) Typhoon Gale Kidneys (Red: New; Purple: Old)

Figure 8: Super Typhoon Mangkhut (1822)

There are also limitations in this new method. Although the method takes the combined effect of TC and other weather systems into consideration, it does not tell which system is dominating the wind situation in Hong Kong. Forecasters may have to rely on real time observation to determine whether TC signals or the Strong Monsoon Signal should be issued.

There are also still many void regions due to insufficient data. The estimated probability values highly rely on interpolation and smoothing. Nevertheless, the interpolation and plotting of the maps were not manually post-processed. Thus, the geometry of the isopleths may not follow the empirical rules as discussed in the Literature Review section. The authenticity of the isopleths may also be limited. It is hoped that the validity of the probability isopleth maps will improve as more TC cases are introduced in the future.

7 Conclusion

In this study, we presented a statistical method to assess the probability of occurrence of strong or gale force winds at Cheung Chau during TC scenarios. Data include track and intensity data of TCs in the SCS in 1993 to 2018 and the corresponding wind speed recorded at Cheung Chau. By stratifying the wind speed data according the corresponding TC intensities, the wind speed data in $1° \times 1°$ grid squares were fit with the Weibull distribution. Using the estimated Weibull parameters, the probability of occurrence of strong or gale force winds at Cheung Chau due to a TC of certain intensity within a grid square could be estimated. Upon interpolation and smoothing, the spatial distributions of the probabilities were presented as probability isopleth maps.

Several TC cases that affected Hong Kong and necessitated the issuance of local TC warning signals were presented. It was found that the geometry of the probability isopleths could reflect the impact of terrain and the semi-circle effect on local wind strength. As northerly winds are sheltered by terrain, the isopleths to the east and southeast of Hong Kong are less extensive and have tight gradients. As Cheung Chau is exposed to east to southeasterly winds, the isopleths are elongated towards the southwest and west. The semi-circle effect also contributes to the amplification of winds from the southeastern

quadrant.

We also analyzed TC cases with different storm sizes. It was found that TCs with large wind radii could lead to early onset of high winds when the TC was still far away from Hong Kong. This was reflected in the probability isopleth maps that strong or gale winds were first observed when the storm track cut the isopleths of lower probability values. The isopleth maps could also account for the strong winds due to the combined effect of the TC and other weather systems including the northeast monsoon and the ridge when the TC departs further from Hong Kong.

There are still some limitations in this method. Although it can cope with TC cases with combined effects, our method is unable to differentiate whether the TC is dominating the wind situation in Hong Kong, which may require manual judgement by weather forecasters. Moreover, insufficient data reduces the reliability of the maps. Manual adjustments may be required to make the map abide by the empirical rules.

This method could be adopted to construct kidneys for newer anemometer stations as one single TC could contribute multiple data in one grid square that could generate sufficient data for analysis despite having fewer TC cases. It is hoped that the maps could be extended to more anaemometer stations in the expanding anaemometer network to assist weather forecasters in assessing the likelihood of strong or gale winds in Hong Kong to issue timely warnings to the general public.

Acknowledgements

This project was completed under the summer placement programme offered by the Hong Kong Observatory. I wish to thank the Department of Physics of The Chinese University of Hong Kong and the Hong Kong Observatory, for offering me the internship in the Observatory and allowing me to apply what I learnt in lessons to practical uses. I am very grateful for having the opportunity to intern at the Observatory, which reaffirmed my interest in meteorology.

I would like to thank Professor Francis Tam, the advisor of my project. He has provided guidelines and suggestions for me to improve my project. I am also very grateful for his full support and encouragement on my work. Without his support, it would not be able for me to explore in the world of meteorology and to discover and learn knowledge that is out of textbooks.

I would like to express my sincere gratitude to Mr. Choy Chun-wing, my project advisor in the Hong Kong Observatory. Despite under the difficult time of the COVID-19 pandemic, he provided his greatest support to my project. His invaluable advice and comments were crucial to the completion of this project. He also let me learn more about tropical cyclone-related knowledge.

I would like to acknowledge Ms. Jessica Acuña, my Language and Communication advisor. She was really helpful in offering advice and comments on the language of this project report. She let me learn more about academic writing and pick up skills in writing a better research paper.

I would like to offer my great appreciation to Dr. Wu Man-chi for his assistance and technical support on this project. He also provided inspiring and valuable comments on the project.

List of Acronyms

BT Best Track

CCH Cheung Chau (Meteorological Station)

CDF Cumulative Distribution Function

EPS Ensemble Prediction System

HKO Hong Kong Observatory

NWP Numerical Weather Prediction

PDF Probability Density Function

SCS South China Sea

SMS Strong Monsoon Signal

ST Severe Typhoon

STS Severe Tropical Storm

Super T Super Typhoon

T/TY Typhoon

TC Tropical Cyclone

TD Tropical Depression

TS Tropical Storm

UTC Coordinated Universal Time

WNP Western North Pacific

References

Aberson, S. D. (2001). The Ensemble of Tropical Cyclone Track Forecasting Models in the North Atlantic Basin (1976–2000). *Bulletin of the American Meteorological Society*, *82*(9), https://journals.ametsoc.org/bams/article-pdf/82/9/1895/3733503/1520-0477(2001)082_0000_teotct_2_3_co_2.pdf, 1895–1904. https://doi.org/10.1175/1520-0477(2001)082<0000:TEOTCT>2.3.CO;2

Ali, S., Lee, S.-M., & Jang, C.-M. (2018). Statistical analysis of wind characteristics using weibull and rayleigh distributions in deokjeok-do island – incheon, south korea. *Renewable energy*, *123*, 652–663.

Azad, K., Rasul, M., Halder, P., & Sutariya, J. (2019). Assessment of wind energy prospect by weibull distribution for prospective wind sites in australia. *Energy procedia*, *160*, 348–355.

Bender, M. A., Marchok, T. P., Sampson, C. R., Knaff, J. A., & Morin, M. J. (2017). Impact of Storm Size on Prediction of Storm Track and Intensity Using the 2016 Operational GFDL Hurricane Model. *Weather and Forecasting*, *32*(4), https://journals.ametsoc.org/waf/article-pdf/32/4/1491/4667848/waf-d-16-0220_1.pdf, 1491–1508. https://doi.org/10.1175/WAF-D-16-0220.1

Bilir, L., İmir, M., Devrim, Y., & Albostan, A. (2015). Seasonal and yearly wind speed distribution and wind power density analysis based on weibull distribution function. *International journal of hydrogen energy*, *40*(44), 15301–15310.

Chin, P. C., & Leong, H. C. (1978). Estimation of wind speeds near sea-level during tropical cyclone conditions in hong kong. http://www.hko.gov.hk/tc/publica/tn/files/tn045.pdf

Doocy, S., Dick, A., Daniels, A., & Kirsch, T. D. (2013). The human impact of tropical cyclones: A historical review of events 1980-2009 and systematic literature review. *PLoS Currents*, *5*. https://doi.org/10.1371/currents.dis.2664354a5571512063ed29d25ffbce74

Elsberry, R. L., & Carr, I., Lester E. (2000). Consensus of Dynamical Tropical Cyclone Track Forecasts—Errors versus Spread. *Monthly Weather Review*, *128*(12),

https://journals.ametsoc.org/mwr/article-pdf/128/12/4131/4188752/1520-0493(2000)129_4131_codtct_2_0_co_2.pdf, 4131–4138. https : / / doi . org/10.1175/1520-0493(2000)129<4131:CODTCT>2.0.CO;2

Gryning, S.-E., Gryning, S.-E., Floors, R., Floors, R., Peña, A., Peña, A., Batchvarova, E., Batchvarova, E., Brümmer, B., & Brümmer, B. (2016). Weibull wind-speed distribution parameters derived from a combination of wind-lidar and tall-mast measurements over land, coastal and marine sites. *Boundary-layer meteorology*, *159*(2), 329–348.

Katopodes, N. D. (2019). Chapter 7 - vorticity dynamics (N. D. Katopodes, Ed.). In N. D. Katopodes (Ed.), *Free-surface flow*. Butterworth-Heinemann. https : / / doi . org / https://doi.org/10.1016/B978-0-12-815489-2.00007-1

Knaff, J. A., & Zehr, R. M. (2007). Reexamination of tropical cyclone wind-pressure relationships. *Weather and forecasting*, *22*(1), 71–88.

Lam, C. C., & Tai, S. C. (2004). Probability forecasts of high winds and related warnings associated with tropical cyclones in hong kong, Guangzhou, China. International Symposium on Tropical Weather and Climate. https://www.hko.gov.hk/tc/publica/reprint/files/r564.pdf

Lam, C. Y. (2000). Tropical cyclone warning system in hong kong, Chiang Mai, Thailand. Regional Technical Conference on Tropical Cyclones and Storm Surges. https : //www.hko.gov.hk/tc/publica/reprint/files/r416.pdf

Lam, K. M., To, A. P., & Guo, D. J. (2006). Wind tunnel study of peak wind pressure on government towers in wanchai during typhoon york 1999. *HKIE Transactions*, *13*(3), https://doi.org/10.1080/1023697X.2006.10668048, 17–22. https://doi.org/10.1080/1023697X.2006.10668048

Lee, T.-C., Knutson, T. R., Kamahori, H., & Ying, M. (2012). Impacts of climate change on tropical cyclones in the western north pacific basin. part i: Past observations. *Tropical Cyclone Research and Review*, *1*(2), 213–235. https : / / doi . org / https : //doi.org/10.6057/2012TCRR02.08

Lee, T.-C., & Ma, C. F. (2004). *Probability of occurrence of gales in the harbour area of hong kong during the passage of tropical cyclones* (tech. rep.). https://www.hko.gov.hk/publica/tnl/tnl081.pdf

Lynch, P. (2008). The origins of computer weather prediction and climate modeling [Predicting weather, climate and extreme events]. *Journal of Computational Physics*, *227*(7), 3431–3444. https://doi.org/https://doi.org/10.1016/j.jcp.2007.02.034

Nam, C. C., Park, D.-S. R., Ho, C.-H., & Chen, D. (2018). Dependency of tropical cyclone risk on track in south korea. *Natural Hazards and Earth System Sciences*, *18*(12), 3225–3234. https://doi.org/10.5194/nhess-18-3225-2018

Ozay, C., & Celiktas, M. S. (2016). Statistical analysis of wind speed using two-parameter weibull distribution in alaçatı region. *Energy conversion and management*, *121*, 49–54.

Properties of the weibull distribution. (2012). In *Using the weibull distribution* (pp. 73–96). John Wiley & Sons, Ltd. https://doi.org/10.1002/9781118351994.ch3

Shu, Z., Li, Q., & Chan, P. (2015). Statistical analysis of wind characteristics and wind energy potential in hong kong. *Energy Conversion and Management*, *101*, 644–657. https://doi.org/https://doi.org/10.1016/j.enconman.2015.05.070

Shum, C.-T., & Or, M.-K. (2012). Case study of typhoon nesat (1117), Macau, China. The 26th Guangdong-Hong Kong-Macau Seminar on Meteorological Science and Technology. http://www.hko.gov.hk/en/publica/reprint/files/r1006.pdf

Sun, Y., Zhong, Z., Yi, L., Li, T., Chen, M., Wan, H., Wang, Y., & Zhong, K. (2015). Dependence of the relationship between the tropical cyclone track and western pacific subtropical high intensity on initial storm size: A numerical investigation. *Journal of Geophysical Research: Atmospheres*, *120*(22), https://agupubs.onlinelibrary.wiley.com/doi/pdf/10.1002/2015JD023716, 11, 451–11, 467. https://doi.org/10.1002/2015JD023716

Ucar, A., & Balo, F. (2009). Evaluation of wind energy potential and electricity generation at six locations in turkey. *Applied energy*, *86*(10), 1864–1872.

Weber, H. C. (2003). Hurricane Track Prediction Using a Statistical Ensemble of Numerical Models. *Monthly Weather Review*, *131*(5),

https://journals.ametsoc.org/mwr/article-pdf/131/5/749/4205857/1520-0493(2003)131_0749_htpuas_2_0_co_2.pdf, 749–770. https : / / doi . org / 10.1175/1520-0493(2003)131<0749:HTPUAS>2.0.CO;2

Yang, M. (2014). Xiaguan xiaoying de fenxi yu yingyong [Analysis and application of the valley effect]. *Dili jiaoxue*, *18*, 43–44.

Zhai, A. R., & Jiang, J. H. (2014). Dependence of US hurricane economic loss on maximum wind speed and storm size. *Environmental Research Letters*, *9*(6), 064019. https://doi.org/10.1088/1748-9326/9/6/064019

Zhang, Z., & Krishnamurti, T. N. (1997). Ensemble Forecasting of Hurricane Tracks. *Bulletin of the American Meteorological Society*, *78*(12), https://journals.ametsoc.org/bams/article-pdf/78/12/2785/3729941/1520-0477(1997)078_2785_efoht_2_0_co_2.pdf, 2785–2796. https : / / doi . org / 10.1175/1520-0477(1997)078<2785:EFOHT>2.0.CO;2